Molecular Crystals and Liquid Crystals
Publication details, including instructions for authors and subscription information:
http://www.tandfonline.com/loi/gmcl18

Flow of a Nematic Liquid Crystal Around a Cylinder

H. Heuer [a] , H. Kneppe [a] & F. Schneider [a]
[a] Physikalische Chemie, Universität Siegen, 5900, Siegen, F. R. Germany
Version of record first published: 04 Oct 2006.

To cite this article: H. Heuer , H. Kneppe & F. Schneider (1991): Flow of a Nematic Liquid Crystal Around a Cylinder, Molecular Crystals and Liquid Crystals, 200:1, 51-70

To link to this article: http://dx.doi.org/10.1080/00268949108044231

Mol. Cryst. Liq. Cryst., 1991, Vol. 200, pp. 51–70
Reprints available directly from the publisher
Photocopying permitted by license only

Printed in the United States of America

Flow of a Nematic Liquid Crystal around a Cylinder

H. HEUER, H. KNEPPE and F. SCHNEIDER

Physikalische Chemie, Universität Siegen 5900 Siegen, F. R. Germany

(Received October 9, 1990; in final form October 26, 1990)

The differential equations for the flow of an incompressible nematic liquid crystal perpendicular to an infinite long cylinder are developed for low Reynolds numbers and a fixed director orientation on the basis of the Leslie-Ericksen theory. Some general results are discussed. The velocities and the force on the cylinder only depend on the shear viscosity coefficients η_1, η_2, and α_1, whereas the pressure additionally depends on the Leslie coefficient α_5. In a "falling cylinder experiment", the cylinder will not fall vertically if the director is neither parallel nor perpendicular to the gravitational field. Numerical calculations are performed with the aid of the artificial compressibility method. Stream line patterns as well as results on pressure and force on the cylinder are presented.

Keywords: Nematic liquid crystal, Leslie-Ericksen equations, hydrodynamics, finite differences

I. INTRODUCTION

The hydrodynamics of nematic liquid crystals can be described by the Leslie-Ericksen theory[1,2] or the theory of the Harvard group.[3] Because of the complexity of these equations, there are only a few examples for which an analytical solution could be found, e.g., flow between parallel plates,[1,4] Couette flow,[5,6] Poiseuille flow,[7] back flow.[8] The determination of more complicated, e.g. three dimensional flow patterns, has not been performed up to now. Especially, the calculation of the flow pattern around a sphere and the evaluation of the analogue to the Stokes formula is an attractive task. On the way to this problem, we have begun with a two dimensional analogue: the flow of a nematic liquid crystal perpendicular to an infinite long cylinder assuming low Reynolds numbers and a fixed director orientation. It is known from the hydrodynamics of isotropic liquids, that the fluid must be bounded, e.g., by a second hollow cylinder.

The differential equations are developed. The evaluation of an analytical solution seems to be impossible for the general case. Besides a discussion of the properties of the differential equations, we have, therefore, used a numerical method (artificial compressibility method[9,10]) to calculate the flow pattern, the pressure and the force on the cylinder.

II. HYDRODYNAMIC EQUATIONS

The basic equations for the flow of a nematic liquid crystal are taken from Leslie and Ericksen using the notation of Clark and Leslie.[11] We assume a fixed director orientation ($\boldsymbol{n}$ = const.) and a weak anchoring at solid surfaces. In this case, the equations reduce for an incompressible nematic liquid crystal and for low Reynolds numbers in the steady case to

$$\sigma_{ij,j} = 0 \tag{1}$$

$$\sigma_{ij} = p\delta_{ij} + \alpha_1 n_k n_p A_{kp} n_i n_j + \alpha_2 N_i n_j + \alpha_3 N_j n_i + \alpha_4 A_{ij} + \alpha_5 A_{ik} n_k n_j + \alpha_6 A_{jk} n_k n_i \tag{2}$$

$$A_{ij} = \tfrac{1}{2}(v_{i,j} + v_{j,i}) \tag{3}$$

$$N_i = \tfrac{1}{2}(v_{j,i} - v_{i,j}) n_j \tag{4}$$

The usual summation convention is used and a comma preceeding a suffix denotes partial differentiation with respect to the following coordinate. The α_i's are the Leslie coefficients of the nematic liquid crystal. The A_{ij}'s are the components of the symmetric part of the velocity gradient tensor. N is the rotation of the director with respect to the fluid. p is the dynamic pressure, i.e. the hydrostatic part of the pressure is omitted.

As our problem is a two-dimensional one (translational symmetry in z direction) there are four non-vanishing components for σ. Simple expressions for these components are obtained if the director is parallel to one of the coordinate axes. For $\boldsymbol{n}$ parallel to the x axis, one obtains

$$\begin{aligned}
\sigma_{xx} &= -p + (\alpha_1 + \alpha_4 + \alpha_5 + \alpha_6) v_{x,x} \\
\sigma_{xy} &= \tfrac{1}{2}(\alpha_3 + \alpha_4 + \alpha_6) v_{x,y} + \tfrac{1}{2}(-\alpha_3 + \alpha_4 + \alpha_6) v_{y,x} \\
\sigma_{yx} &= \tfrac{1}{2}(\alpha_2 + \alpha_4 + \alpha_5) v_{x,y} + \tfrac{1}{2}(-\alpha_2 + \alpha_4 + \alpha_5) v_{y,x} \\
\sigma_{yy} &= -p + \alpha_4 v_{y,y}
\end{aligned} \tag{5}$$

Insertion in Equation (1) and employing the continuity equation

$$v_{x,x} + v_{y,y} = 0 \tag{6}$$

leads to

$$-[p - (\tfrac{1}{2}\alpha_1 + \alpha_5) v_{x,x}]_{,x} + \eta_2 \Delta v_x + \tfrac{1}{2}\alpha_1 v_{x,xx} = 0 \tag{7}$$

$$-[p - (\tfrac{1}{2}\alpha_1 + \alpha_5) v_{x,x}]_{,y} + \eta_1 \Delta v_y + \tfrac{1}{2}\alpha_1 v_{y,yy} = 0 \tag{8}$$

where the η_i are the shear viscosity coefficients

$$\eta_1 = \tfrac{1}{2}(-\alpha_2 + \alpha_4 + \alpha_5) \tag{9}$$

$$\eta_2 = \tfrac{1}{2}(\alpha_3 + \alpha_4 + \alpha_6) \tag{10}$$

and Δ is the two-dimensional Laplace operator.

Equations (6), (7), and (8) are the basic equations for our problem. Inspection of the Equations (7) and (8) shows that the coefficient combination $\frac{1}{2}\alpha_1 + \alpha_5$ does influence the pressure but not the velocities, if the coefficients η_1, η_2, and α_1 are kept constant. Therefore, p and $(\frac{1}{2}\alpha_1 + \alpha_5)v_{x,x}$ can be lumped together in a new pressure variable

$$p' = p - (\tfrac{1}{2}\alpha_1 + \alpha_5)v_{x,x} \tag{11}$$

The problem can be solved with this modified pressure p' and the real pressure can be calculated later on. Furthermore, Equations (7) and (8) can be divided by one of the viscosity coefficients, e.g. η_2. The resulting equations show that the velocities and the reduced pressure p'/η_2 only depend on the ratios α_1/η_2 and η_1/η_2.

Equations (7) and (8) are the most symmetric presentation of the differential equations. Obviously, it is possible to cancel the α_1 terms in Equation (8) and to integrate the two α_1 terms in Equation (7) in one term. Although this presentation is shorter, we prefer the symmetric presentation, as an important simplification in the numerical calculation later on is only possible in this presentation.

After introduction of p', Equations (7) and (8) differ from the isotropic case by the different shear viscosity coefficients and the α_1 term. η_1 and η_2 are the viscosity coefficients for a director orientation parallel to the velocity gradient and parallel to the flow velocity, resp. They become equal in an isotropic liquid. α_1 is an additional viscosity coefficient which plays a role when the director orientation is neither parallel to the flow velocity nor parallel to the velocity gradient. It is usually a small term and vanishes for isotropic liquids.

It is known that there is no solution for the creeping flow which satisfies the boundary conditions when a cylinder is moved perpendicular to its long axis in an unbounded isotropic liquid (Stokes' paradox). The dimensional analysis of the problem shows that there must be a second length besides the diameter of the moving cylinder. This length can be introduced by a second hollow cylinder which gives an outer boundary for the liquid.

We have, therefore, studied the steady creeping flow of an incompressible nematic liquid crystal with fixed director orientation around an infinite long cylinder under the following boundary conditions:

velocity at the inner cylinder $\boldsymbol{v}_i = 0$,

velocity at the outer coaxial cylinder $\boldsymbol{v}_0 = \text{const.}$

and perpendicular to the cylinder axes.

The two boundary conditions can be interchanged in principle and we shall use in the following the short hand notation: motion of the outer cylinder or the inner cylinder.

Both cases lead to some difficulties with respect to the coaxial position of the cylinders in an experiment with a real movement. Further difficulties arise from the assumed fixed director orientation which can be accomplished in principle by application of a magnetic field of sufficient strength. Two effects lead to deviations from the assumed fixed director orientation. Firstly, the director orientation in the bulk is determined within a magnetic coherence by the orientation of the director at the surfaces of the cylinders, as a surface with a weak anchoring can not be prepared. If we assume a homeotropic surface alignment, elastic torques and forces on the cylinders cancel due to symmetry. The flow pattern is changed within the region of the coherence length. The largest deviation takes place in y direction as the calculation assumes an effective viscosity coefficient η_2 in this direction whereas η_1 is effective in an experiment. Usually, η_1 exceeds η_2 and we assume the worst case $\eta_1 \to \infty$. This case can be described by a local increase of the inner cylinder radius and a decrease of the outer one by one coherence length which is approximately 1 μm in a field of 3 T, i.e. the influence of this effect can be neglected if the radius of the inner cylinder and the difference to the outer radius exceed e.g. 1 mm.

Secondly, there is a torque on the director which is caused by the shear flow. This torque and the magnetic torque lead to an equilibrium orientation of the director. The influence of this effect can be neglected under usual experimental conditions.

Because of the translational symmetry in z direction the problem is a two-dimensional one and the two-dimensional formulation would be: motion of a disc in a two-dimensional liquid crystal which is bounded by a concentric circle of large diameter.

The system of differential Equations (6), (7), and (8) is linear. If, therefore, two solutions are known, e.g. for the cases

$$\boldsymbol{v}_0 \text{ parallel to } \mathbf{n}$$

and

$$\boldsymbol{v}_0 \text{ perpendicular to } \mathbf{n}$$

it is possible to calculate the solution for the general boundary condition $\boldsymbol{v}_0 = (v_0 \cos\psi, v_0 \sin\psi)$, where ψ is the angle between $\boldsymbol{v}_0$ and the x axis, by a superposition of these two solutions:

$$\boldsymbol{v} = \cos\psi\, \boldsymbol{v}_{\parallel} + \sin\psi\, \boldsymbol{v}_{\perp} \tag{12}$$

$$p = \cos\psi\, p_{\parallel} + \sin\psi\, p_{\perp} \tag{13}$$

$$\boldsymbol{F} = \cos\psi\, \boldsymbol{F}_{\parallel} + \sin\psi\, \boldsymbol{F}_{\perp} \tag{14}$$

where the suffixes $_{\parallel}$ and $_{\perp}$ denote the solutions for the parallel and the perpendicular case. F, the force per unit length on the inner cylinder, can be resolved into a component parallel ($F^{\parallel}$) and a component perpendicular ($F^{\perp}$) to $\boldsymbol{v}_0$:

$$F^{\parallel} = \cos^2\psi\, F_{\parallel} + \sin^2\psi\, F_{\perp} \tag{15}$$

$$F^{\perp} = \sin\psi \cos\psi\, (F_{\parallel} - F_{\perp}) \tag{16}$$

It should be noticed that the force on the cylinder is not parallel to the velocity at the outer cylinder if this velocity does not coincide with one of the coordinate axes. Especially, a cylinder will not fall vertically in a gravitational field (reversed boundary conditions) if the director is neither parallel nor perpendicular to this field. Numerical examples for the deviation are given later on.

The two different solutions which are necessary for the calculation of the general solution by superposition can be obtained by a simplified procedure. The solution for the case $\boldsymbol{v}_0$ perpendicular to $\boldsymbol{n}$ can be obtained by interchanging x and y in Equations (7) and (8) and using the boundary condition $\boldsymbol{v}_0$ parallel to $\boldsymbol{n}$

$$-[p - (\tfrac{1}{2}\alpha_1' + \alpha_5')v_{y,y}]_{,y} + \eta_2'\Delta v_y + \tfrac{1}{2}\alpha_1' v_{y,yy} = 0 \tag{17}$$

$$-[p - (\tfrac{1}{2}\alpha_1' + \alpha_5')v_{y,y}]_{,x} + \eta_1'\Delta v_x + \tfrac{1}{2}\alpha_1' v_{x,xx} = 0 \tag{18}$$

With the aid of the continuity equation (6), the term with the mixed differentiation can be transformed in order to get the same derivatives as in the original equation.

$$-(p + (\tfrac{1}{2}\alpha_1' + \alpha_5')v_{x,x})_{,y} + \eta_2'\Delta v_y + \tfrac{1}{2}\alpha_1' v_{y,yy} = 0 \tag{19}$$

$$-(p + (\tfrac{1}{2}\alpha_1' + \alpha_5')v_{x,x})_{,x} + \eta_1'\Delta v_x + \tfrac{1}{2}\alpha_1' v_{x,xx} = 0 \tag{20}$$

A comparison with Equations (7) and (8) gives

$$\eta_1' = \eta_2$$

$$\eta_2' = \eta_1$$

$$\alpha_1' = \alpha_1$$

$$\tfrac{1}{2}\alpha_1' + \alpha_5' = -(\tfrac{1}{2}\alpha_1 + \alpha_5) \tag{21}$$

i.e., the calculation for the boundary condition $\boldsymbol{v}_0$ perpendicular to $\boldsymbol{n}$ can be performed by a calculation with the boundary condition $\boldsymbol{v}_0$ parallel to $\boldsymbol{n}$ with the set of viscosity coefficients given in Equation (21) and a subsequent rotation of the solution by 90°. This allows a simpler numerical calculation later on, as both calculations can now be performed on a quadrant of the grid using the same symmetry properties.

The boundary conditions suggest the use of a polar coordinate system for the

calculation. Furthermore, the unequal distribution of the velocity gradients, i.e. strong gradients at the inner cylinder and small gradients at the outer suggest a non-linear radial coordinate. We have, therefore, used a logarithmic polar coordinate system[12] in which the variables ϕ and ζ are defined by

$$\tan \phi = y/x; \qquad \zeta = \ln (r/r_i) \tag{22}$$

where r_i is the radius of the inner cylinder. The corresponding transformation of the velocity components was not performed as the resulting expressions become very long. After a multiplication by $r_i \cdot e^{\zeta}$ the transformed equations are

$$- \cos\phi\, P'_{,\zeta} + \sin\phi\, P'_{,\varphi} + e^{-\zeta}(V_{x,\zeta\zeta} + V_{x,\varphi\varphi}) + \frac{\alpha_1}{2\eta_2 e^{\zeta}}(\cos^2\phi\, V_{x,\zeta\zeta} - \sin 2\phi\, V_{x,\zeta\varphi} + \sin^2\phi\, V_{x,\varphi\varphi} - \cos 2\phi\, V_{x,\zeta} + \sin 2\phi\, V_{x,\varphi}) = 0 \tag{23}$$

$$- \sin\phi\, P'_{,\zeta} - \cos\phi\, P'_{,\varphi} + \frac{\eta_1}{\eta_2 e^{\zeta}}(V_{y,\zeta\zeta} + V_{y,\varphi\varphi}) + \frac{\alpha_1}{2\eta_2 e^{\zeta}}(\sin^2\phi\, V_{y,\zeta\zeta} + \sin 2\phi\, V_{y,\zeta\varphi} + \cos^2\phi\, V_{y,\varphi\varphi} + \cos 2\phi\, V_{y,\zeta} - \sin 2\phi\, V_{y,\varphi}) = 0 \tag{24}$$

$$\cos\phi\, V_{x,\zeta} - \sin\phi\, V_{x,\varphi} + \sin\phi\, V_{y,\zeta} + \cos\phi\, V_{y,\varphi} = 0 \tag{25}$$

where the dimensionless quantities P' and V are defined by

$$P' = \frac{p' r_i}{\eta_2 v_0} \quad \text{and} \quad V = \frac{v}{v_0} \tag{26}$$

For a comparison later on we present the analytical solution for an isotropic liquid. The general solution for the stream function is known to be

$$\Psi = \sin\phi\,(A \cdot r + B \cdot r^{-1} + C \cdot r^3 + D \cdot r \cdot \ln r) \tag{27}$$

The unknown constants A, B, C, and D are evaluated from the boundary condition $v_i = 0$ and $\mathbf{v}_0 = (v_0, 0)$.

$$v_r = v_0 \cos\phi\,[(1 + R_0^2)\ln R + \tfrac{1}{2}(1 - R^2) - \tfrac{1}{2}R_0^2(1 - R^{-2})]/f(R_0) \tag{28}$$

$$v_\varphi = -v_0 \sin\phi\,[(1 + R_0^2)\ln R + \tfrac{3}{2}(1 - R^2) + \tfrac{1}{2}R_0^2(1 - R^{-2})]/f(R_0) \tag{29}$$

where

$$f(R_0) = 1 - R_0^2 + (1 + R_0^2)\ln R_0 \quad \text{and} \quad R = r/r_i \tag{30}$$

The pressure can be determined by an integration of the differential equation for v_r or v_φ.

$$p = -\frac{2\eta v_0 \cos\phi}{r \cdot f(R_0)} (1 + R_0^2 + 2R^2) \tag{31}$$

III. DETERMINATION OF THE FORCE ON THE INNER CYLINDER

As the general solution can be obtained by a superposition of the solutions for $V_0 = (1,0)$ and $V_0 = (0,1)$ and the latter can be determined from the case $V_0 = (1,0)$ with the modified set of viscosity coefficients (Equation 21), we only have to calculate the force F_x in x direction for the case V_0 parallel to n. The force differential is given by

$$dF_x = \cos\phi\, dF_\zeta - \sin\phi\, dF_\varphi = (\cos\phi\, \sigma_{\zeta\zeta} - \sin\phi\, \sigma_{\varphi\zeta}) dS_\zeta \tag{32}$$

where S_ζ is the only non-vanishing component of the surface normal of the inner cylinder. The tensor components $\sigma_{\zeta\zeta}$ and $\sigma_{\varphi\zeta}$ are obtained from the cartesian tensor components by

$$\sigma_{\zeta\zeta} = \cos^2\phi\, \sigma_{xx} + \sin\phi \cos\phi\, (\sigma_{xy} + \sigma_{yx}) + \sin^2\phi\, \sigma_{yy} \tag{33}$$

$$\sigma_{\varphi\zeta} = \sin\phi \cos\phi\, (-\sigma_{xx} + \sigma_{yy}) - \sin^2\phi\, \sigma_{xy} + \cos^2\phi\, \sigma_{yx} \tag{34}$$

Insertion in Equation (32), insertion of the tensor components (5), and transformation of the velocity components into the components v_φ and v_ζ in logarithmic polar coordinates leads to

$$dF_x = -[\cos\phi\, p + r_i^{-1} \sin\phi\, v_{\varphi,\zeta}(\eta_2 + (\alpha_1 + \alpha_5)\cos^2\phi)] dS_\zeta \tag{35}$$

at the surface of the inner cylinder. Integration around the cylinder gives

$$F_x/l = -\int_0^{2\pi} [r_i \cos\phi\, p + \sin\phi\, v_{\varphi,\zeta}(\eta_2 + (\alpha_1 + \alpha_5)\cos^2\phi)] d\phi \tag{36}$$

where F_x/l is the force per unit length of the inner cylinder. Introduction of the modified pressure p' (see Equation (11)) leads to

$$F_x/l = -\int_0^{2\pi} [r_i \cos\phi\, p' + (\eta_2 + \tfrac{1}{2}\alpha_1)\sin\phi\cos^2\phi\, v_{\varphi,\zeta}] d\phi \tag{37}$$

Using dimensionless quantities and taking into account the symmetry of the problem, the integral reads as

$$F_x/l = -4\eta_2 v_0 \int_0^{\pi/2} [\cos\phi\, P' + \sin\phi(1 + \frac{\alpha_1}{2\eta_2} \cos^2\phi)\, V_{\varphi,\zeta}] d\phi \tag{38}$$

The force on the inner cylinder for an isotropic liquid can be calculated by means of Equation (36) with $\eta_2 = \eta$ and $\alpha_1 = \alpha_5 = 0$ using v_φ from Equation (29).

$$F_x/l = \frac{4\pi\eta v_0}{\ln R_0 + \dfrac{1 - R_0^2}{1 + R_0^2}} \tag{39}$$

IV. FINITE DIFFERENCE EQUATIONS

As the system of differential Equations (23), (24), and (25) is rather complex in the derivatives, only simple finite difference schemes can be applied. The simplest scheme for the evaluation of the steady flow of an incompressible liquid is used in the artificial compressibility method (AC method).[9,10] Usually, the marker-and-cell (MAC) mesh is used. This mesh typ, however, leads to difficulties with the boundary conditions in our case as the velocities V_x and V_y are not perpendicular to the boundaries. We have, therefore, used a mesh in which only the pressure points are staggered. Figure 1 shows the grid with a small number of meshes. Velocities and pressures for the missing part of the grid are given by symmetry.

In the AC method, the steady state is calculated from a system of time dependent

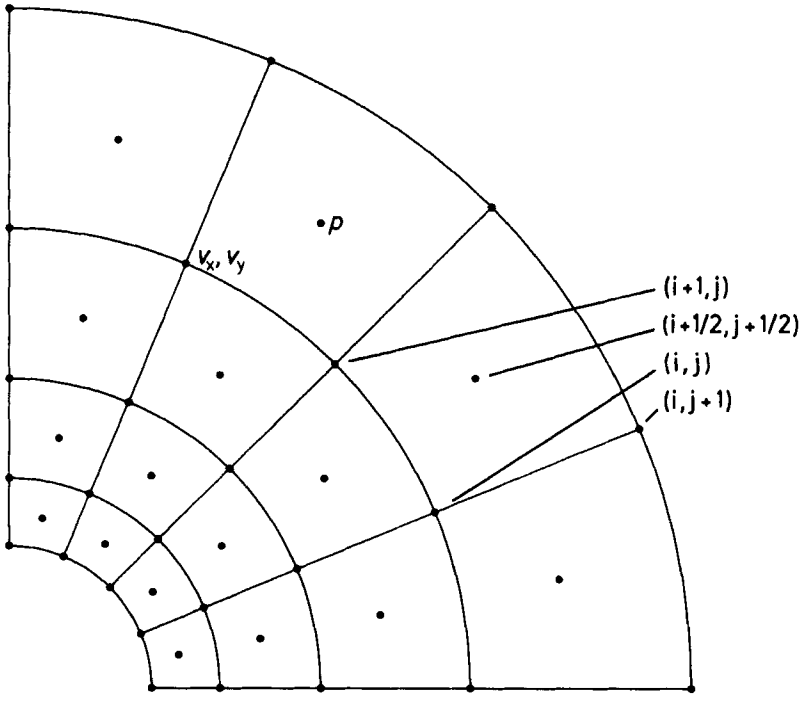

FIGURE 1 Grid for the numerical calculation.

equations for $t \to \infty$. The time dependent equations for Equations (23), (24), and (25) become

$$V_{x,T} = -\cos\phi\, P'_{,\zeta} + \sin\phi\, P'_{,\varphi} + e^{-\zeta}(V_{x,\zeta\zeta} + V_{x,\varphi\varphi}) + \frac{\alpha_1}{2\eta_2 e^{\zeta}}(\cos^2\phi\, V_{x,\zeta\zeta} - \sin 2\phi\, V_{x,\zeta\varphi} + \sin^2\phi\, V_{x,\varphi\varphi} - \cos 2\phi\, V_{x,\zeta} + \sin 2\phi\, V_{x,\varphi}) \quad (40)$$

$$V_{y,T} = -\sin\phi\, P'_{,\zeta} - \cos\phi\, P'_{,\varphi} + \frac{\eta_1}{\eta_2 e^{\zeta}}(V_{y,\zeta\zeta} + V_{y,\varphi\varphi}) + \frac{\alpha_1}{2\eta_2 e^{\zeta}}(\sin^2\phi\, V_{y,\zeta\zeta} + \sin 2\phi\, V_{y,\zeta\varphi} + \cos^2\phi\, V_{y,\varphi\varphi} + \cos 2\phi\, V_{y,\zeta} - \sin 2\phi\, V_{y,\varphi}) = 0 \quad (41)$$

$$P'_{,T} = -C^2(\cos\phi\, V_{x,\zeta} - \sin\phi\, V_{x,\varphi} + \sin\phi\, V_{y,\zeta} + \cos\phi\, V_{y,\varphi}) \quad (42)$$

where the dimensionless time is defined by $T = tv_0/r_i$. Equation (42) results from the time dependent continuity equation for a fluid with an artificial equation of state $p = c^2 \cdot \ln \rho$. c^2 is the inverse compressibility which is transformed by a multiplication with $r_i/\eta_2 v_0$ into the dimensionless quantity C^2. This constant has to be chosen for optimum convergence. The factor $1/r_i \cdot e^{\zeta}$ which has been dropped in Equations (23), (24), and (25) has been omitted further on, as the convergence of the numerical calculations was better without this factor.

As the space and time discretization of the equations leads to rather long expressions, we only describe the discretization method. Time derivatives were replaced by

$$\frac{f^{n+1} - f^n}{\Delta T} \quad (43)$$

where n denotes the time level. Space derivatives in Equations (40) and (41) were replaced by central differences

e.g.

$$V_{x,\zeta}: \quad (V_x^n(i, j+1) - V_x^{n+1}(i, j-1))/2\Delta\phi \quad (44)$$

$$V_{x,\zeta\zeta}: \quad (V_x^n(i, j+1) - 2V_x^n(i, j) + V_x^{n+1}(i, j-1))/\Delta\phi^2 \quad (45)$$

$$V_{x,\zeta\varphi}: \quad (V_x^n(i+1, j+1) - V_x^n(i-1, j+1) - V_x^{n+1}(i+1, j-1) + V_x^{n+1}(i-1, j-1))/4\Delta\phi^2 \quad (46)$$

$$P_{,\zeta}: \quad (P^n(i+\tfrac{1}{2}, j+\tfrac{1}{2}) - P^n(i+\tfrac{1}{2}, j-\tfrac{1}{2}) + P^n(i-\tfrac{1}{2}, j+\tfrac{1}{2}) - P^n(i-\tfrac{1}{2}, j-\tfrac{1}{2}))/2\Delta\phi \quad (47)$$

where $\Delta\phi = \Delta\zeta$ is assumed. The first term in the parentheses denotes the point number in ϕ and the second in ζ direction (see Figure 1). The different time levels in the space discretization result from an overwriting technique.[10] As soon as a velocity at level $n + 1$ is calculated, it is used for subsequent calculations. This accelerates the convergence, allows a greater time step and saves memory. The scheme is entirely explicit, if ϕ is changed in the innermost loop. The pressure at time level $n + 1$ is calculated after every full cycle over the velocities. The space derivatives at the pressure points $(i + \frac{1}{2}, j + \frac{1}{2})$ (Equation (42)) were replaced by

$$V_{x,\zeta}: \quad (V_x^{n+1}(i + 1, j + 1) - V_x^{n+1}(i + 1, j) + V_x^{n+1}(i, j + 1) - V_x^{n+1}(i, j))/2\Delta\phi \quad (48)$$

The error in the space derivatives is $O(\Delta\phi^2)$ and in the time derivatives $O(\Delta T)$. The minor precision in the time derivatives is sufficient as we are only interested in the steady state solution. The boundary conditions are

$$V_x = 0 \text{ at the inner cylinder}$$

$$V_x = 1 \text{ at the outer cylinder}$$

$$V_y = 0 \text{ at the periphery of the quadrant}$$

The velocities V_x for $\phi = 0$ and $\pi/2$ have to be calculated. Values at neighbour points which do not lie in the quadrant are given by symmetry

$$V_x(\phi, \zeta) = V_x(-\phi, \zeta); \qquad P(\phi, \zeta) = P(-\phi, \zeta)$$

$$V_x(\phi, \zeta) = V_x(\pi - \phi, \zeta); \qquad P(\phi, \zeta) = -P(\pi - \phi, \zeta) \quad (49)$$

All pressure values to be calculated lie in the quadrant. There is no need for any reflection technique or extrapolation for the calculation of points near the boundary.

The numerical calculations were started with the solution for an isotropic liquid. The convergence is strongly influenced by the choice of ΔT and C^2. The employment of the AC method is limited by a very restrictive criterion for numerical stability. Small mesh sizes and high viscosity coefficients only allow the employment of very small time steps. The evaluation of a general criterion for numerical stability was not possible because of the complex differential equations and boundary conditions. Numerical experiments for the most important case $\alpha_1 << (\eta_1, \eta_2)$ showed that the differential equation with the higher Laplace operator coefficient restricts the maximum time step. The analogue

$$\frac{2\Delta T \cdot \text{Max}(1, \eta_1/\eta_2)}{\Delta\phi^2} \leq 1 \quad (50)$$

to the classical parabolic criterion for overwriting and equal grid distances turned out to be a good guideline for the choice of ΔT. Usually, a ΔT was chosen which led to a value of 0.5–0.7. As long as

$$\frac{\Delta T C^2}{\text{Max}(1, \eta_1/\eta_2)} < 1 \tag{51}$$

the time step limit is not significantly influenced by C^2. A precise choice of C^2 is unnecessary as the convergence shows a broad optimum as a function of C^2. Usually, the chosen C^2 led to a value of 0.1–0.5. If C^2 is significantly greater, numerical instabilities occur which can not be suppressed by a corresponding reduction in ΔT.

The number of time steps needed for the determination of the steady state solution depends on the anisotropy of the viscosity coefficients. For our standard grid (25 points in ϕ direction between 0 and $\pi/2$, 41 points in ζ direction, and $r_0/r_i = 13.708$), $\eta_1/\eta_2 = 10$, and $\alpha_1 = 0$ about 20 000 time steps were needed.

The calculation of the force on the inner cylinder according to Equation (38) demands P' and $V_{\varphi,\zeta}$ at the inner cylinder. P' was determined by an extrapolation over $\frac{1}{2}\Delta\zeta$ using the pressure at the four innermost points of the staggered grid. $V_{\varphi,\zeta}$ was determined by an unsymmetrical numerical differentiation also using four points. The numerical integration was performed for the first quadrant taking into account equal weights for an integration from $\phi = 0$ to 2π.

The accuracy of the calculation is determined by the error $O(\Delta\phi^2)$ of the space derivatives. For our standard grid, the errors in the pressure at the stem point and in the force are smaller than 0.25%. This was shown for the case $\eta_1/\eta_2 = 1$ and $\alpha_1 = 0$ by a comparison with the isotropic solution. For the anisotropic case, it was shown by a plot of the interesting quantity versus $\Delta\phi^2$ and extrapolation to $\Delta\phi = 0$.

The numerical calculations were performed on a personal computer with an 80 386/387 processor and on a VAX 8820.

V. RESULTS

At first, we want to present some characteristic stream line patterns. Figures 2 and 3 show the stream lines for a movement of the outer cylinder using our standard cylinder configuration with $r_0/r_i = 13.708$ and the standard grid described above. In order to visualize the influence of the viscosity coefficients, a large anisotropy of the coefficients was chosen: $\eta_1/\eta_2 = 10$ for Figure 2 and $\eta_1/\eta_2 = 0.1$ for Figure 3; $\alpha_1 = 0$ for both cases. Such large anisotropies can be observed under special circumstances. $\eta_1 > \eta_2$ is the usual relation and ratios of $\eta_1/\eta_2 = 8.25$ were observed for the eutectic mixture of 4-methoxy-4′-n-butyl-azoxybenzenes.[13] Even larger ratios should be observed for liquid crystals with broader nematic phase ranges. $\eta_1 < \eta_2$ is observed in some nematic phases just above a transition to a smectic phase and probably in nematic phases of discotic liquid crystals. Values up to $\eta_2/\eta_1 =$

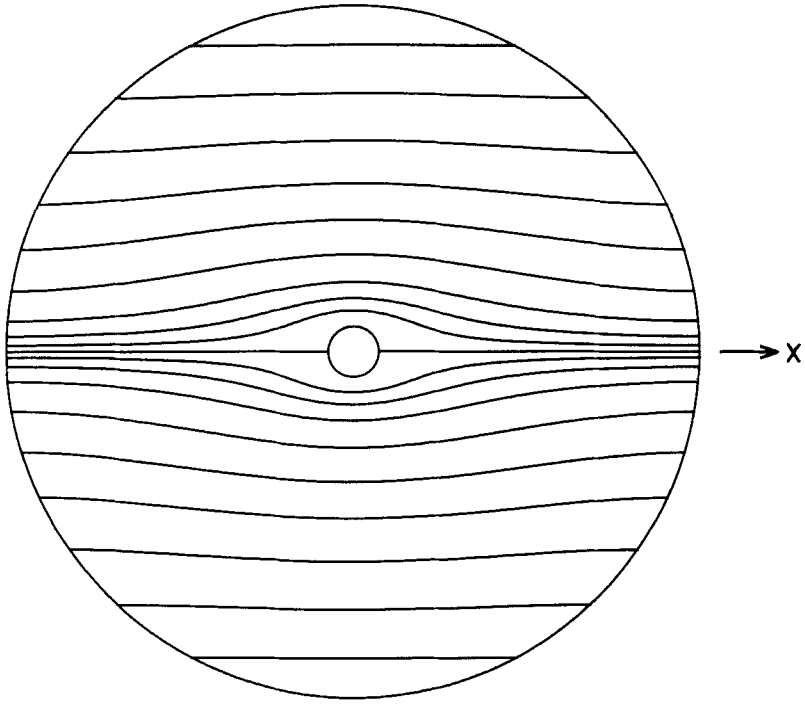

FIGURE 2 Streamline pattern for a nematic liquid crystal with the viscosity coefficient ratios $\eta_1/\eta_2 = 10$ and $\alpha_1 = 0$. The director orientation is parallel to the x axis. The nematic liquid crystal is bounded by two concentric cylinders with a radii ratio of 13.708 and the outer cylinder is moved parallel to the x axis. The long cylinder axes are perpendicular to the drawing plane. A more detailed description of the boundary conditions is given in the text.

20 have been observed for a reentrant mixture of cyanobiphenyl compounds[14] and the ratio should diverge at the transition.

The characteristic course of the stream lines can be understood by means of a minimum principle. In the case of incompressible isotropic liquids, the resulting steady flow at low Reynolds numbers dissipates the minimum of energy for given boundary conditions. The same principle is valid for the flow of nematic liquid crystals as shown in the following. The dissipation function for an incompressible nematic liquid crystals is[15]

$$D = \frac{\alpha_4}{4}(v_{i,j}v_{i,j} + v_{i,j}v_{j,i}) + \frac{\alpha_5 - \alpha_2}{4}(n_i v_{k,j} - \dot{n}_k)(n_j v_{k,i} - \dot{n}_k)$$

$$+ \frac{\alpha_6 + \alpha_3}{4}(n_i v_{i,k} + \dot{n}_k)(n_j v_{j,k} + \dot{n}_k)$$

$$+ \frac{\alpha_6 - \alpha_3}{2}(n_i v_{k,i} - \dot{n}_k)(n_j v_{j,k} + \dot{n}_k) + \frac{\alpha_1}{2} n_i n_j n_k n_l v_{i,j} v_{k,l} \quad (52)$$

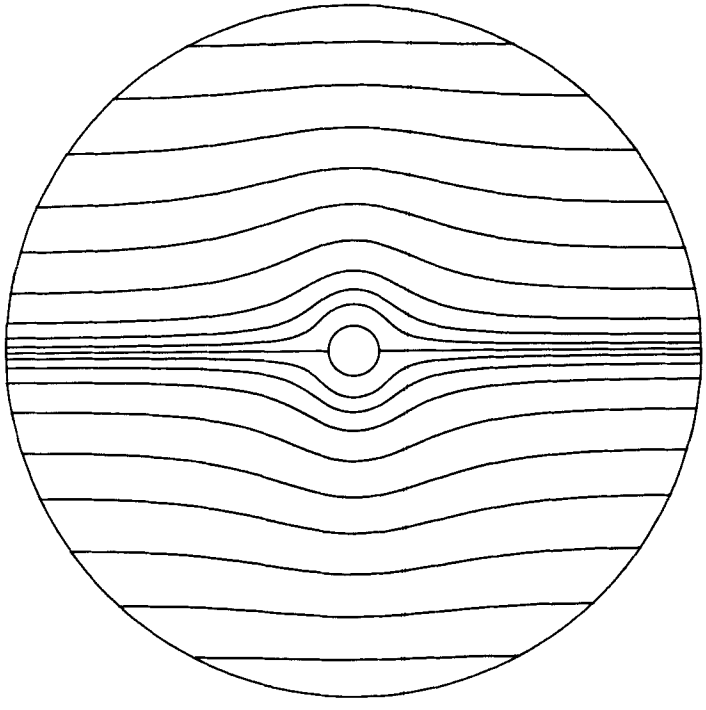

FIGURE 3 Stream line pattern for $\eta_1/\eta_2 = 0.1$ and $\alpha_1 = 0$. Further description as in Figure 2.

$\dot{n}$ disappears in the steady case. Furthermore, we set $n = (1,0)$ without loss of generality.

$$D = \frac{\alpha_4}{4}(v_{i,j}v_{i,j} + v_{i,j}v_{j,i}) + \frac{\alpha_5 - \alpha_2}{4} v_{i,x}v_{i,x} + \frac{\alpha_6 + \alpha_3}{4} v_{x,i}v_{x,i} + \frac{\alpha_6 - \alpha_3}{2} v_{i,x}v_{x,i} + \frac{\alpha_1}{2}v_{x,x}^2 \quad (53)$$

The energy dissipation per unit length of the fluid volume with the cross section A is now

$$\int_A D dx dy \quad (54)$$

The minimum energy dissipation is determined by means of the Euler equations

$$\frac{\partial D^*}{\partial v_i} - \frac{\partial}{\partial x}\frac{\partial D^*}{\partial v_{i,x}} - \frac{\partial}{\partial y}\frac{\partial D^*}{\partial v_{i,y}} = 0, \; i = x \text{ and } y \quad (55)$$

with

$$D^* = D + \lambda(x, y) \cdot v_{j,j} \quad (56)$$

where $\lambda(x, y)$ is an unknown function. Insertion of the dissipation function (53) leads to the differential Equations (7) and (8) with $\lambda = -p$, i.e. the solutions of the Leslie-Ericksen equations under the assumptions discussed above lead to a flow with a minimum energy dissipation. The effective viscosity coefficient η_{eff} for a nematic liquid crystal with an arbitrary angle ϑ between director and flow velocity is

$$\eta_{\text{eff}} = \eta_1 \sin^2\vartheta + \eta_2 \cos^2\vartheta + \alpha_1 \sin^2\vartheta \cos^2\vartheta \tag{57}$$

provided that the director lies in the shear plane. Therefore, η_1 is effective near the left hand and right hand part of the inner and outer cylinder; η_2 near the upper and lower part. $\eta_1 > \eta_2$ leads, therefore, to a flow which avoids large areas with strong gradients at the left hand and right hand part of the inner cylinder and vice versa. Figures 4 and 5 show the corresponding stream lines for a movement of the inner cylinder. The explanation of the differences in the stream line patterns is the same as for the movement of the outer cylinder.

Figure 6 shows the reduced pressure

$$P^* = [p - (\tfrac{1}{2}\alpha_1 + \alpha_5)v_{x,x}]r_i/\sqrt{\eta_1\eta_2}v_0 \tag{58}$$

at the inner cylinder for a movement of the outer cylinder. This reduced pressure

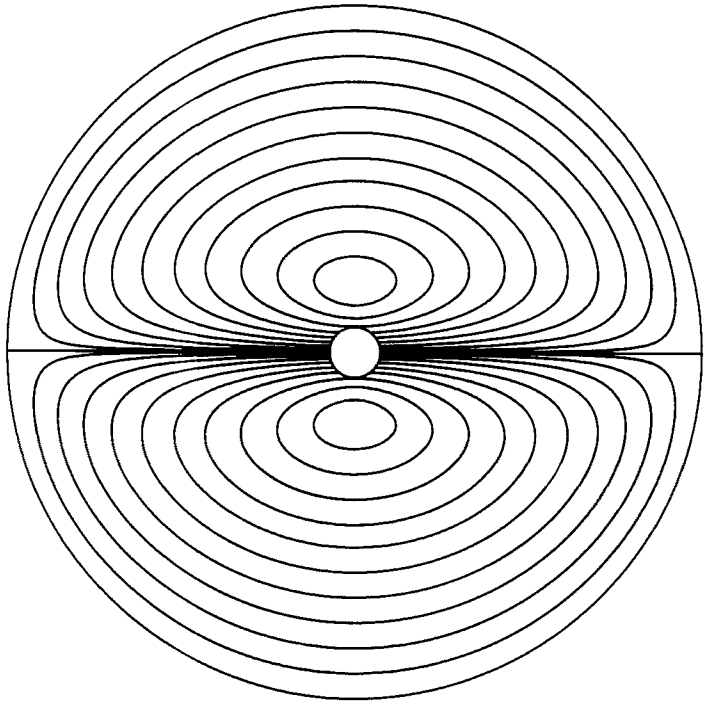

FIGURE 4 Stream line pattern for a movement of the inner cylinder. Further description as in Figure 2.

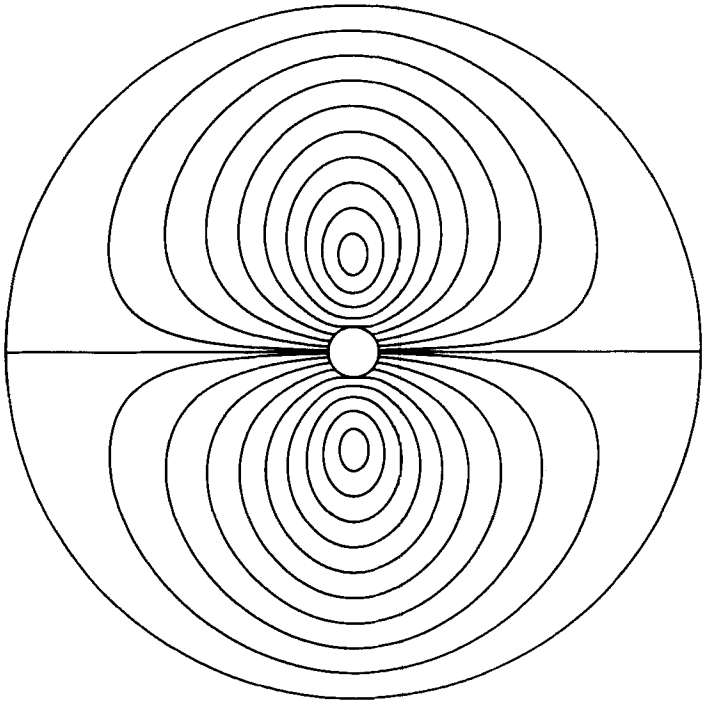

FIGURE 5 Stream line pattern for a movement of the inner cylinder. Further description as in Figure 3.

is slightly modified as compared with P' in order to give a better presentation in the figure. As compared with the cosϕ function of an isotropic liquid, a liquid crystal with a viscosity coefficient ratio of $\eta_1/\eta_2 = 10$ gives a strong enhancement of the pressure at angles between 45 and 90°. This is caused by the plug like flow for $\eta_1/\eta_2 = 10$. The reversed anisotropy leads to a concentration of the flow around the x axis which gives the strong enhancement of P^* in this area. In order to get the real pressure, $(\frac{1}{2}\alpha_1 + \alpha_5)\, V_{x,x}$ has to be added. Whereas $\alpha_1/2$ is usually a small quantity, e.g. $\eta_1 = 0.19$, $\eta_2 = 0.031$, $\eta_3 = 0.055$, $\alpha_1 = -0.022$, $\alpha_5 = 0.11$, and $\alpha_6 = -0.047$ Pa s for 4-methoxybenzylidene-4′-n-butyl-aniline (MBBA) at 20°C,[16] the effect of α_5 can not be neglected. A rough estimate of α_5 from η_1 and η_2 is possible with the aid of the following calculation. Subtraction of Equation (10) from (9) gives

$$\eta_1 - \eta_2 = \tfrac{1}{2}(\alpha_5 - \alpha_6 - \alpha_2 - \alpha_3) = \alpha_5 - \alpha_6 \tag{59}$$

where the last part is obtained by application of the Parodi relation

$$\alpha_6 - \alpha_5 = \alpha_2 + \alpha_3 \tag{60}$$

which connects four of the Leslie coefficients. With the assumption $\alpha_6 \approx -\frac{1}{2}\alpha_5$ which is approximately valid for MBBA, $\alpha_5/\eta_2 = \frac{2}{3}(\eta_1/\eta_2 - 1)$ results.

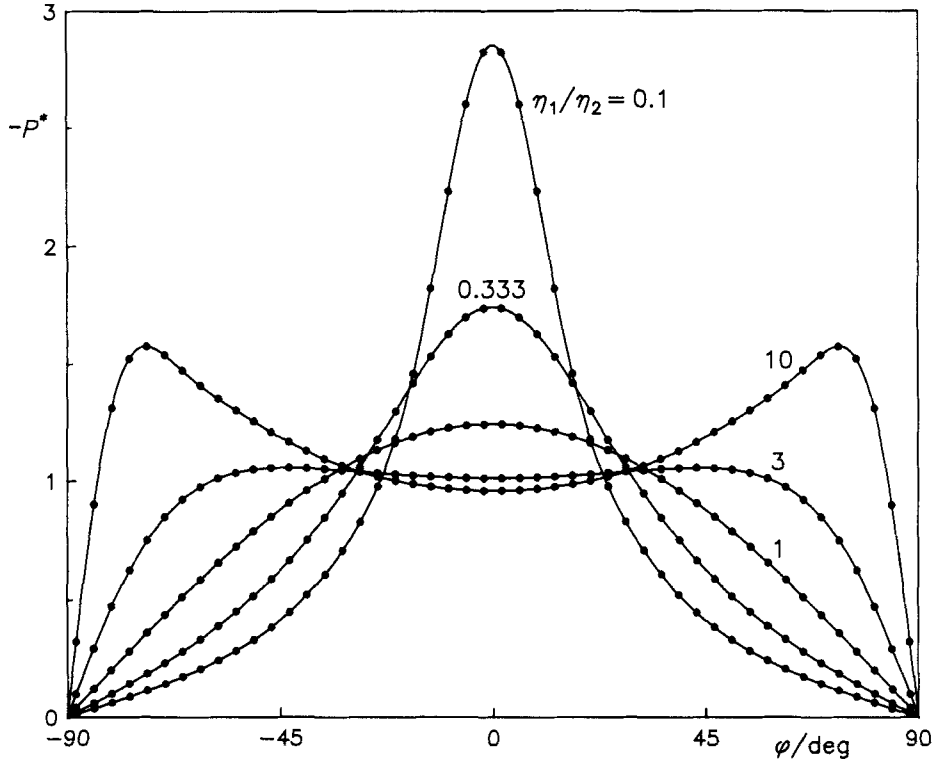

FIGURE 6 Reduced pressure P^* (see text) at the surface of the inner cylinder as a function of the angle ϕ for a movement of the outer cylinder for different viscosity coefficient ratios η_1/η_2.

The velocity gradient $V_{x,x} = -\sin\phi\cos\phi \cdot V_{\varphi,\xi}$ changes around the cylinder and vanishes at the stem point and at $\phi = 90°$. The maximum value of about 0.5 depends only slightly on η_1/η_2 and is observed at about $\phi = 75°$ for $\eta_1/\eta_2 = 10$ and $\phi = 30°$ for $\eta_1/\eta_2 = 0.1$ as determined by the numerical calculations. The addition of the $(\frac{1}{2}\alpha_1 + \alpha_5)\, V_{x,x}$ term, which is positive for $\eta_1/\eta_2 > 1$, to the negative pressure leads to a decrease around the two maxima. A detailed numerical calculation with a set of data for $\eta_1/\eta_2 = 10$ on a 49/81 point grid showed that the two maxima disappear but the pressure exceeds the isotropic values in this region considerably. A calculation of the real pressure for the reversed anisotropy is impossible, as reliable Leslie coefficients are missing.

Figure 7 shows the stream line pattern for a movement of the outer cylinder which is not parallel to one of the coordinate axes. As the director ($\boldsymbol{n} \parallel x$) is now under an oblique angle to the movement of the outer cylinder, the mirror symmetry of the flow with respect to the direction of the movement disappears. This pattern can also be understood by means of the minimum principle. The stream lines beginning at an angle $> 45°$ come nearer to the inner cylinder in the first quadrant than those beginning at $< 45°$, as the small viscosity coefficient η_2 is effective above the inner cylinder and the greater coefficient η_1 is effective at the right hand part of the inner cylinder. On the other side of the cylinder, the circumstances are

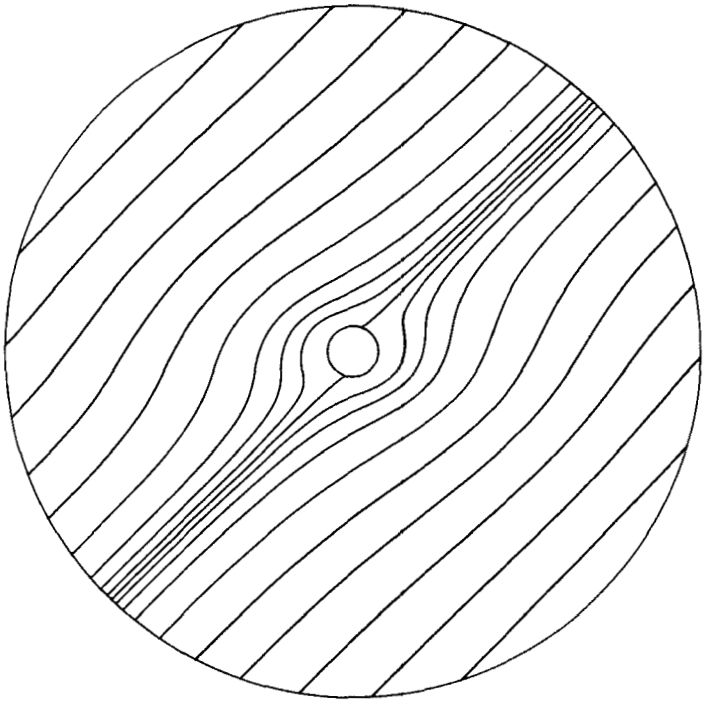

FIGURE 7 Stream line pattern for a movement of the outer cylinder under 45°. The viscosity coefficient ratios are $\eta_1/\eta_2 = 10$ and $\alpha_1 = 0$. Further description as in Figure 2.

reversed. The asymmetry of the stream line pattern leads to a force component perpendicular to the movement of the outer cylinder.

As the viscosity coefficient α_1 is usually small as compared with the other coefficients (see above), there is nearly no change in the stream line pattern as compared with $\alpha_1 = 0$. In order to show the effect of α_1 on the stream line pattern, larger values have to be used. Large negative values are not allowed, as the effective viscosity coefficient (Equation 57) must be positive. We have, therefore, used a large positive value for the following calculation. Because of the $\sin^2\vartheta \cos^2\vartheta$ term, $\alpha_1/\eta_2 = 40$ leads to a comparable anisotropy as assumed for η_1/η_2 in the cases discussed above. The stream line pattern for the case $\eta_1/\eta_2 = 1$ and $\alpha_1/\eta_2 = 40$ is very similar to that in Figure 2. The reason is that the α_1 term becomes effective at $\vartheta = 45°$. The resulting flow pattern contains, therefore, no areas in which a strong gradient is coupled with stream lines under 45° to the coordinate axes. A more specific argument can be derived from the dissipation function (53) in which the α_1 term is of the form $0.5\alpha_1 v_{x,x}^2$. This is now the dominating term for the energy dissipation. As the boundary condition demands $v_x = 0$ at the inner cylinder, $v_{x,x} \approx 0$ leads to very small v_x values in the area around $\phi = 0$ and 180°.

A remarkable stream line pattern occurs for a movement of the inner cylinder under 45° to the x axis (Figure 8). The peculiar stream lines are caused by the condition $v_{x,x} = -v_{y,y} \approx 0$. As v_x and v_y disappear at the vortex centers, there must be a vertical line to the periphery for which v_y disappears and a horizontal

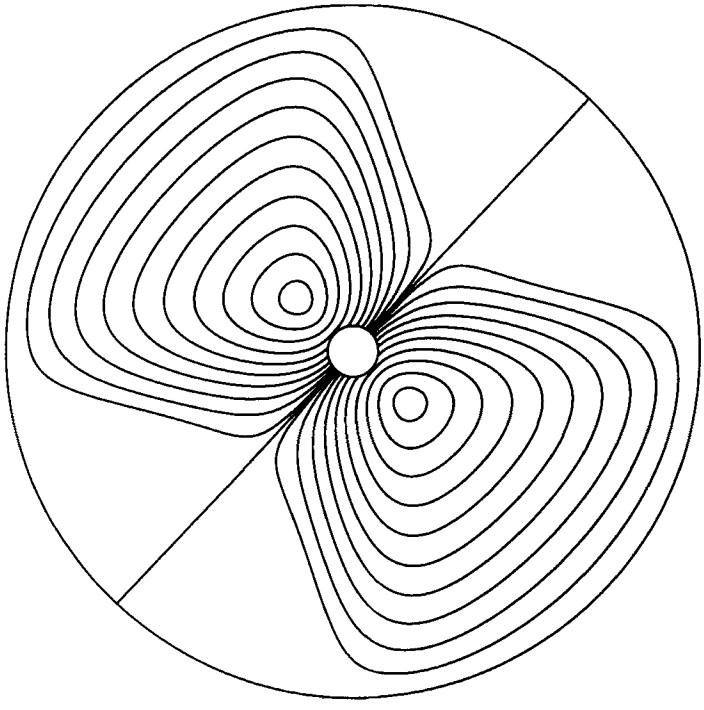

FIGURE 8 Stream line pattern for a movement of the inner cylinder under 45°. The viscosity coefficient ratios are $\eta_1/\eta_2 = 1$ and $\alpha_1/\eta_2 = 40$. Further description as in Figure 2.

line for which v_x disappears. Owing to this effect the corners in the stream lines appear. The conditions $v_x, v_y = 0$ are not fulfilled for the other lines from the vortex center to the inner cylinder as the symmetry of the problem demands a flow under 45°.

In the following we want to discuss some results on the force on the inner cylinder. Inspection of the force integral (38) and the differential Equations (23), (24), and (25) shows that there must exist an equation of the form

$$\frac{F_x}{\eta_2 l v_0} = f\left(\frac{\eta_1}{\eta_2}, \frac{\alpha_1}{\eta_2}, \frac{r_0}{r_i}\right) \tag{61}$$

for the dimensionless quantities of the problem. We have performed numerical calculations for the two radii ratios $R_0 = r_0/r_i = 13.708$ and 4.810, resp. and $\alpha_1 = 0$. In order to allow a better comparison of the two calculations, the force was normalized with respect to the force in the isotropic case

$$F^* = \frac{F_x}{4\pi\eta_2 l v_0}\left(\ln R_0 + \frac{1 - R_0^2}{1 + R_0^2}\right) \tag{62}$$

The plot (Figure 9) versus the square root of the viscosity coefficient ratio η_1/η_2

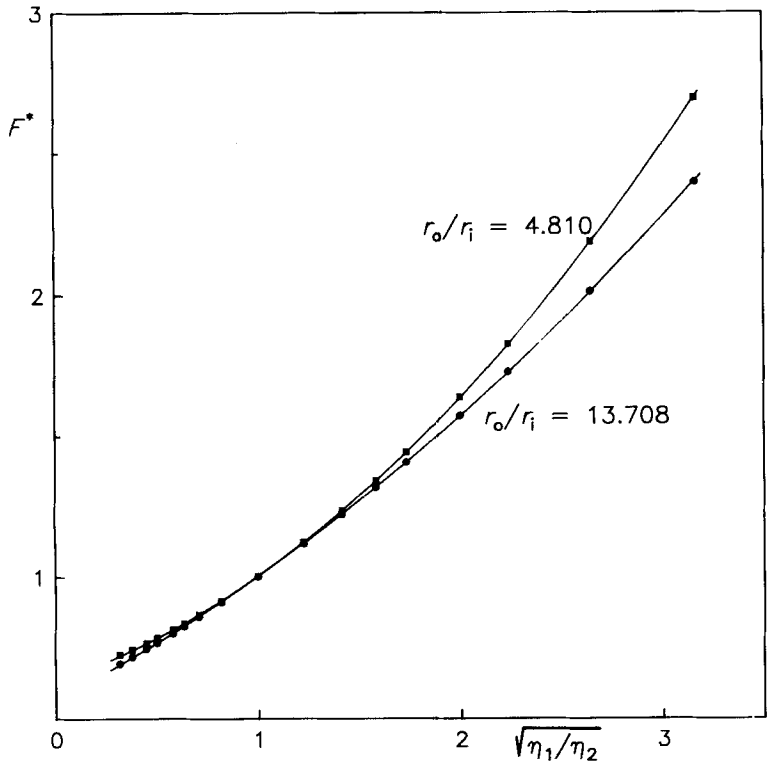

FIGURE 9 Force F^* on the inner cylinder in a normalized form versus the square root of the viscosity coefficient ratio η_1/η_2 for the two radii ratios R_0 = 13.708 and 4.810, resp.

gives a better resolution at low ratios. An equation for the dependence $F^* = g(\eta_1/\eta_2)$ was not found. However, it should be noticed that an equation of the form

$$F^* = A + B(\eta_1/\eta_2)^\alpha \tag{63}$$

with α = 0.67 and 0.81 for R_0 = 13.708 and 4.810, resp., represents the force with a precision of some percent over the dynamic range from η_1/η_2 = 0.1 to 10.

The strong anisotropy of the viscosity coefficients of nematic liquid crystals leads to a big force perpendicular to the movement if the director is neither parallel nor perpendicular to the direction of movement. In the following, we want to discuss the falling direction of a cylinder in a gravitational field. Simple trigonometric arguments allow to derive an equation for the angle β between gravitational field and falling direction for arbitrary angles γ between director and gravitational field:

$$\tan\beta = \frac{-F^\perp}{F^\parallel} = \frac{\sin(\gamma - \beta)\cos(\gamma - \beta)(F_\perp - F_\parallel)}{\cos^2(\gamma - \beta)F_\parallel + \sin^2(\gamma - \beta)F_\perp}$$

$$= \frac{\tan(\gamma - \beta)(F_\perp/F_\parallel - 1)}{1 + \tan^2(\gamma - \beta)F_\perp/F_\parallel} \tag{64}$$

An example for the order of magnitude of the effect is given for the radii ratio $r_0/r_i = 13.708$, the viscosity coefficient ratio $\eta_1/\eta_2 = 10$, and $\alpha_1 = 0$. Two numerical calculations of F_x/l, which are already contained in the data for Figure 9, with the ratios $\eta_1/\eta_2 = 10$ and $\eta_1/\eta_2 = 0.1$ lead to the force ratio $F_\perp/F_\parallel = 2.903$. For a fixed value of $\gamma = 45°$, we find $\beta = 26°$ and the maximum β value is 29.2° at $\gamma = 59.6°$. The greater β value for higher γ values results from the fact that the angle between director and cylinder velocity decreases by the oblique falling direction. For the reversed anisotropy $\eta_1/\eta_2 = 0.1$, the maximum deviation occurs at the complementary angle, i.e. at the smaller γ value of 30.4°, as the perpendicular force increases the angle between director and falling direction. Besides the reversed sign, the β value is the same as above. It should be noticed that a real movement of the inner cylinder would violate the assumed coaxial position of the cylinders.

In a subsequent paper, we shall study the axisymmetrical and the general three-dimensional flow of a nematic liquid crystal around a sphere.

Acknowledgment

The financial support by the Deutsche Forschungsgemeinschaft is gratefully appreciated.

References

1. F. M. Leslie, *Arch. Ratl. Mech. Anal.*, **28**, 265 (1968).
2. J. L. Ericksen, *Mol. Cryst. Liq. Cryst.*, **7**, 153 (1969).
3. D. Forster, T. C. Lubensky, P. C. Martin, J. Swift and P. S. Pershan, *Phys. Rev. Lett.*, **26**, 1016 (1971).
4. P. K. Currie, *J. Physique*, **40**, 501 (1979).
5. R. J. Atkin and F. M. Leslie, *Q. J. Mech. Appl. Math.*, **23**, S3 (1970).
6. P. K. Currie, *Arch. Ratl. Mech. Anal.*, **37**, 222 (1970).
7. R. J. Atkin, *Arch. Ratl. Mech. Anal.*, **38**, 224 (1970).
8. P. Pieransky, F. Brochard and E. Guyon, *J. Physique*, **34**, 35 (1973).
9. A. J. Chorin, *J. Comp. Phys.*, **2**, 12 (1967).
10. R. Peyret and Th. D. Taylor, Computational methods for fluid flow, Springer 1983, p. 144.
11. M. G. Clark and F. M. Leslie, *Proc. R. Soc. Lond.* A, **361**, 463 (1978).
12. B. Fornberg, *J. Fluid. Mech.*, **98**, 819 (1980).
13. H. Kneppe, F. Schneider and N. K. Sharma, *Ber. Bunsenges. Phys. Chem.*, **85**, 784 (1981).
14. S. Bhattacharya and S. V. Letcher, *Phys. Rev. Lett.*, **44**, 414 (1980).
15. G. Vertogen and W. H. de Jeu, *Thermotropic liquid crystals*, Fundamentals, Springer 1988, p. 140.
16. H. Kneppe, F. Schneider and N. K. Sharma, *J. Chem. Phys.*, **77**, 3203 (1982).